Unidirectional Dimerization and Stacking of Ureidopyrimidinone End Groups in Polycaprolactone Supramolecular Polymers

D. J. M. van Beek,[†] A. J. H. Spiering,[†] Gerrit W. M. Peters,[‡] Klaas te Nijenhuis,[§] and Rint P. Sijbesma*,[†]

Laboratory of Macromolecular and Organic Chemistry, Eindhoven University of Technology, Eindhoven, The Netherlands, Materials Technology Institute, Department of Mechanical Engineering, Eindhoven University of Technology, Eindhoven, The Netherlands, and Laboratory of Polymer Materials and Polymer Engineering, Faculty of Applied Sciences, Delft University of Technology, Delft, The Netherlands

Received June 4, 2007; Revised Manuscript Received August 31, 2007

ABSTRACT: The effect of stacking of end groups on the rheological behavior of supramolecular polymer melts is reported. Oscillatory shear experiments in the transition zone from the pseudo rubber plateau to the flow region of telechelic polycaprolactones (PCLs) with ureidopyrimidinone (UPy) end groups directly attached to PCL can be fitted with a single Maxwell element. This demonstrates that dimerization of the UPy groups is unidirectional and that reversible chain scission is faster than reptation. If the UPy groups are connected to the polymer via a urethane linker, a low-frequency plateau in G' is observed. This is ascribed to the formation of a network of stacked UPy dimers, aided by urethane hydrogen bonding. Below their melting point, these stacks form long fibers in the urethane linked supramolecular poly(methyl caprolactone), which were observed with atomic force microscopy (AFM). Steric hindrance interferes with stacking, since the plateau in G' is lower in a urethane linked polymer with bulky adamantyl−UPy end groups.

1. Introduction

Supramolecular polymers,[1−4] polymers in which the monomeric units are held together by noncovalent interactions, form a novel class of materials, which has aroused considerable fundamental and practical interest. These polymers combine many properties of covalent polymers with those of low molecular weight materials, due to the reversibility of the noncovalent interactions. Many different kinds of interactions such as metal coordination, hydrophobic, van der Waals, or electrostatic interactions have been used to form supramolecular polymers. However, in the design of stable supramolecular polymers, employing arrays of multiple hydrogen bonds is probably the strategy with the best prospects for applications.[5] Following the pioneering work of Lehn[6,7] and co-workers on the use of triple hydrogen bonds, supramolecular polymers based on three,[8] four,[9,10] or more[11−16] hydrogen bonds have been reported. In our laboratory, ureidopyrimidinone (UPy, Scheme 1) was developed as a self-complementary quadruple hydrogen-bonding unit with a high dimerization constant ($K_{dim} = 6 \times 10^7$ M^{-1} in $CHCl_3$).[10,17] UPy has been used extensively by us and by others as a binding unit for supramolecular polymers.[10,18−21] Its synthetic accessibility, and the ease with which small molecules[22−24] as well as telechelic polymers,[20,25,26] e.g., poly(ethylene butylene) (PEB),[18,27] can be functionalized with UPy moieties to form supramolecular polymers with a wide range of properties, promise to enable the transformation of supramolecular polymers from a scientific curiosity to a concept with a wide range of practical applications.[5]

The growth of applications of UPy-based supramolecular polymers further enhances the importance of a thorough understanding of the relation between chemical structure and mechanical properties of supramolecular polymers. In the past, we have emphasized the importance of unidirectionality of hydrogen bonding in order to establish supramolecular polymers as a class of materials directly analogous to linear covalent polymers. Properties of UPy-based supramolecular polymers in solution, particularly the concentration dependent viscosities, show excellent agreement with the predictions of the theoretical model of Cates.[28] This model was developed to describe the properties of a specific type of linear supramolecular polymers: solutions of wormlike micelles.[29−31] It predicts the dynamics of entangled supramolecular polymers in the framework of the reptation model by taking into account the breaking and recombination of unidirectionally associating sticky end groups.

Parallel to the development of linear supramolecular polymers, strong multidirectional hydrogen-bonding units have been developed by Stadler et al. [32−34] to form networks in polymeric materials as supramolecular analogues of cross-linked polymers, and the dynamic properties of these materials have been investigated theoretically with the "sticky reptation" model.[35−37]

Scheme 1. Dimer of Ureidopyrimidinone (UPy)

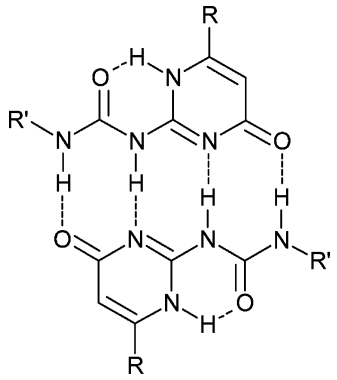

* Corresponding author. E-mail: R.P.Sijbesma@tue.nl.
[†] Laboratory of Macromolecular and Organic Chemistry, Eindhoven University of Technology.
[‡] Department of Mechanical Engineering, Eindhoven University of Technology.
[§] Delft University of Technology.

10.1021/ma0712394 CCC: $37.00
Published on Web 10/20/2007

Scheme 2. Hydroxy-telechelic Polycaprolactones PCL 2k and PCL 80k, and UPy-telechelic Polycaprolactones 1, 2, 3, and 4

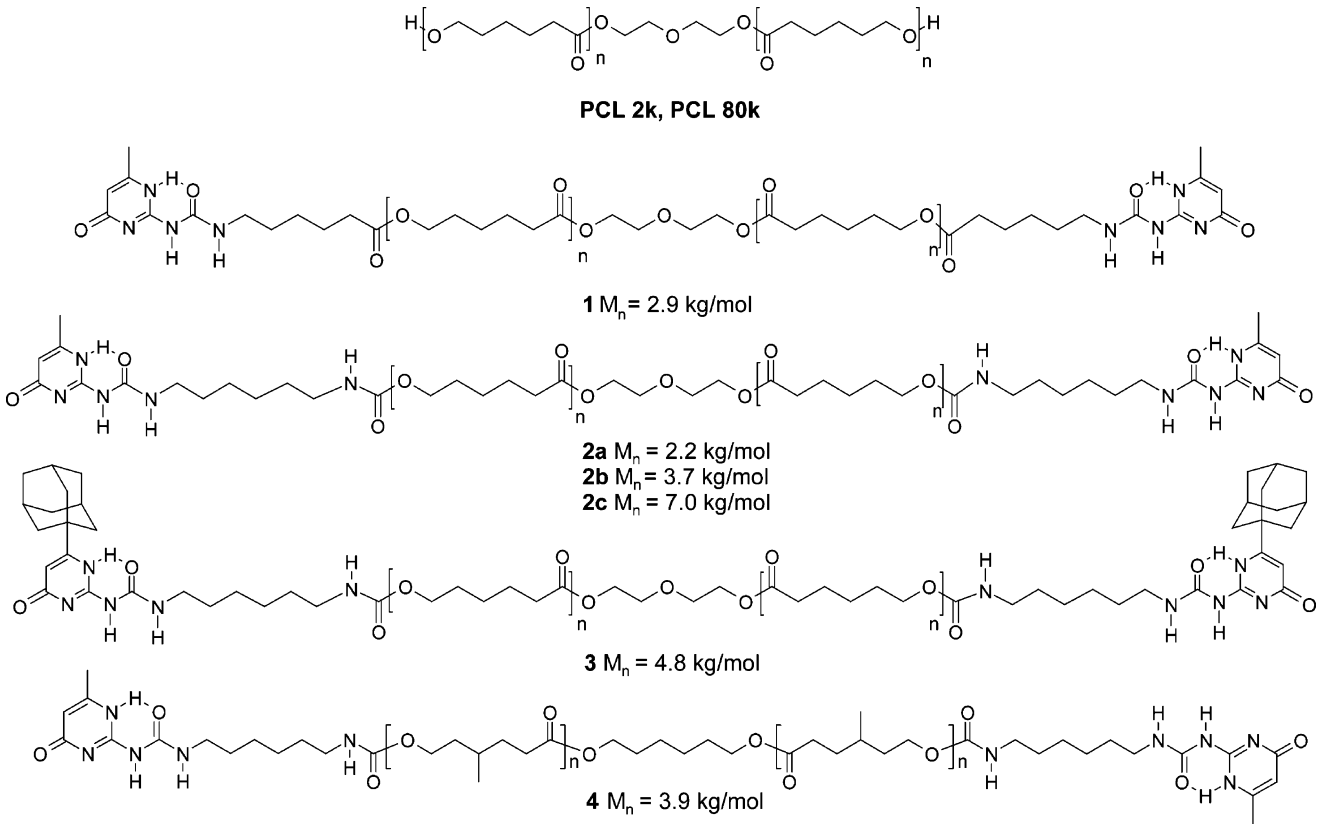

UPy-based supramolecular polymeric materials prepared from telechelic polymers by functionalization with UPy synthons[18,25,27,38,39] are promising candidates for applications. The rheology of the melt state of such UPy-telechelic polymers is more complex[40,41] than for unidirectionally associated telechelic monomers or for the coordinatively cross-linked polymer networks described by Craig[42−44] and co-workers. Unusual rheological behavior was observed by Rowan[45] and co-workers when they examined poly(THF) functionalized with modified adenine and cytosine. Although the association constant between the nucleobases is very low ($<5\ M^{-1}$), materials with film and fiber-forming capabilities were obtained. Whereas the cytosine-modified polymer resulted in a critical gel over a large temperature range, the material properties of the adenine-modified polymer were shown to be temperature dependent. Between 50 and 90 °C, thermorheologically simple behavior was observed, complying with TTS. The observed plateau modulus was higher than expected, and the lack of terminal viscosity suggested extremely long relaxation times. The long living interactions were proposed to orginate from phase separation between the polymer backbone and $\pi-\pi$ stacking of the adenine units. Increasing the temperature up to 100 °C resulted in characteristic gel behavior, visualized by parallel lines in a plot of log G' and log G'' against frequency, whereas above a temperature of 130 °C, loss of the polymer-like properties was observed for both modified polymers.

The complex rheology of supramolecular structures suggests that multiple relaxation processes are operative. In particular the presence of a plateau in the storage (G') modulus at lower frequencies suggests that an understanding of the molecular background of the behavior of these materials should include multidirectional association of the UPy units in the melt as well. Indeed, UPy groups have been shown to aggregate strongly beyond the dimeric state in UPy-telechelic poly(ethylene butylene)[27] to form long fibers, which enhances their mechanical properties. The formation of fibers was proposed to result from stacking of the UPy groups, which is aided by hydrogen bonding of urethane or urea groups next to the UPy units.

In order to study the effects of stacking in polar polymers and at higher temperatures, we decided to compare the rheology of UPy telechelic polycaprolactone (PCL) derivatives. Supramolecular polymers based on PCL are biocompatible and biodegradable, and the functionality can be introduced in a modular way.[25,46] Surface morphologies of several supramolecular PCL derivatives have been investigated by atomic force microscopy and have shown the presence of fibers at room temperature.[47]

Unfunctionalized PCL is a semicrystalline material, which is flexible at room-temperature due to its low glass transition temperature ($T_g = -60$ °C) and which melts above 60 °C.[48] This polymer has important applications as a biomaterial.[49]

In the present paper, we report on the rheology of low molecular weight UPy-telechelic polycaprolactone derivatives **1**−**4** (Scheme 2). The high sensitivity of rheology for network formation allows us to investigate the effects of variations in structure and molecular weight on stacking in unprecedented detail. Structural variations include the absence or presence of a urethane group close to the UPy end groups in compounds **1** and **2**, respectively; the length of the polymeric linker in polymers **2a**−**2c**, and the presence of a bulky adamantyl substituent on the UPy end groups in **3**. The rheology of these compounds is compared with that of their high molecular weight covalent counterpart (**PCL 80k**). Since the semicrystalline nature of the polycaprolactone supramolecular polymers displays mainly crystalline platelets in AFM phase images,[47] a UPy telechelic polymer with an amorphous linker (poly(methyl caprolactone)) is used to study surface morphology with AFM. All polymers are fully characterized by differential scanning calorimetry (DSC) and variable temperature infrared spectros-

copy (VT-IR). The rheological behavior is analyzed within the framework of Cates' theory for polymer **1** and with the use of a reversible network model for polymers **2**−**4**.

2. Experimental Section

2.1. Chemicals. High molecular weight polycaprolactone (**PCL 80k**; M_n = 80 kg/mol, PDI 1.55) was used as received from Aldrich. Low molecular weight hydroxytelechelic polycaprolactone (**PCL 2k**; M_n = 2 kg/mol, PDI 1.8) was used as received from Acros. Hydroxytelechelic polycaprolactone with molecular weights of 1 and 4 kg/mol were prepared by ring opening polymerization of ϵ-caprolactone (Aldrich) using tin(II) 2-ethylhexanoate (Aldrich) and diethylene glycol (Acros) as initiator. 4-Methyl-caprolactone was obtained by a Baeyer−Villiger oxidation as described in the literature.[50] Hydroxytelechelic poly(methyl-caprolactone) was prepared by ring opening polymerization of 4-methyl-caprolactone using hexane diol (Acros) as initiator and fumaric acid (Acros) as catalyst (see the Supporting Information). Deuterated chloroform was obtained from Cambridge Isotope Laboratories, Inc., and all other solvents were obtained from Biosolve. Hexafluoroacetone and α,α,α-trifluorotoluene were obtained from ABCR and Aldrich, respectively. All chemicals were used without further purification unless stated otherwise.

2.2. Characterization. ^{1}H NMR and ^{13}C NMR spectra were recorded on a Varian Mercury 200, Varian Gemini 300 or Varian Mercury 400 and ^{19}F NMR spectra were recorded on a Varian Mercury 400 spectrometer. ^{1}H and ^{13}C chemical shifts are reported in ppm relative to tetramethylsilane (TMS). ^{19}F NMR spectra were measured with a sweep width of 11295 Hz, acquisition time of 15 s and a relaxation delay of 15 s. ^{19}F chemical shifts are reported in ppm relative to C_6F_6 but were actually measured relative to α,α,α-trifluorotoluene (TFT), δ = −64.00 ppm, as internal standard. Infrared (IR) spectra were recorded on a Perkin-Elmer Spectrum One FT-IR spectrometer with a Universal ATR Sampling Accessory for solids. Gel permeation chromatography (GPC) was performed on a Shimadzu LC-10ADvp, using a Shimadzu SPD-M10Avp foto diode array detector at 254 nm and a PLgel 5 μm Mixed C (200−2 × 10^6 g/mol) column in serie with a PLgel 5 μm Mixed D (200−4·10^5 g/mol) column. THF was used as mobile phase (1 mL/min, room temperature) and polystyrene standards were used for calibration. Sample concentrations were 1−3 mg/mL in the eluent solvent.

2.3. Differential Scanning Calorimetry (DSC). DSC measurements were performed on a Perkin-Elmer differential scanning calorimeter Pyris 1 with DSC Autosampler and Perkin-Elmer CCA7 cooling element under a nitrogen atmosphere with heating and cooling rates of 10 K/min (T_m) or 40 K/min (T_g). Samples of 8−12 mg were measured.

2.4. Preparation of HFA Adducts for End Group Titration with ^{19}F NMR. Hexafluoroacetone (HFA) gas was dissolved in dry $CDCl_3$ (4 Å molsieves) using standard Schlenk techniques. The solution was stored at −8 °C over 4 Å mol sieves. The solution contained a mixture of free HFA ($(CF_3)_2$−CO) and its water adduct ($(CF_3)_2$−CO·H_2O), due to the presence of traces of water. ^{19}F NMR (376.5 MHz, $CDCl_3$): δ = −76.31 ppm (s, $(CF_3)_2$−CO) and −83.65 ppm (s, $(CF_3)_2$−CO·H_2O).

A ^{19}F NMR sample of the HFA adduct of the hydroxyl groups of **PCL 2k** and ureidopyrimidone functionalized polycaprolactone derivatives was prepared by adding 0.3 mL of HFA (0.2 mM) solution in $CDCl_3$ to a solution of 15−50 mg of **PCL 2k** or polycaprolactone derivatives in 1 mL of $CDCl_3$ dried on molsieves. 5 μL of α,α,α-trifluorotoluene was added as internal standard.

2.5. Variable Temperature Infrared Spectroscopy. Attenuated total reflection infrared (ATR-IR) spectroscopy was measured on small polymer films using a BioRad Excalibur 3000 spectrometer equipped with a Specac Golden Gate ATR setup. The IR spectra were recorded over a spectral range of 650 up to 4000 cm^{-1} with a resolution of 4 cm^{-1} co-adding 8 scans. Spectra were recorded after 3 min of equilibration upon reaching the desired temperature. For temperature calibration, benzyl (Reichert, Vienna, T_m = 95 °C), phenyl ether (Fluka, T_m = 27 °C), biphenyl (Across, T_m = 68 °C), and benzoic acid (Merck, T_m = 122 °C) were used as reference compounds. All given temperatures are corrected using this calibration.

2.6. Rheology. Oscillatory shear experiments were performed on a Rheometrics ARES over a broad range of temperatures (70−130 °C) and angular frequencies ω (0.001−500 rad/s). In each measurement, the applied strain was maintained at a constant nominal value within the linear viscoelastic range, determined with strain sweeps. The measurements were performed using parallel plate geometry, maintaining a distance between the plates of approximately 1 mm. Specimens with dimensions of 25 and 50 mm diameter were used, for which values of the moduli in a range of 10−2 to 10^6 Pa could be measured. All experiments were carried out under nitrogen atmosphere to avoid thermo-oxidative degradation. The characteristic viscoelastic functions, storage modulus (G'), loss modulus (G''), and complex viscosity ($|\eta^*|$) have been obtained for different temperatures. Low values in the storage moduli of some of the measured polymers lead to scattering in the tan δ, which prohibited time−temperature superposition (TTS) using the tan δ curves as refernce curve. The use of G'' curves as reference curves for TTS resulted in representative curves and were therefore used in all cases. In a frequency range of 1−100 rad/s, the horizontal shift factor a_T was determined and applied on the measured frequency regime at a reference temperature of 50 °C for **4**, 110 °C for **2c**, and at 70 °C for all other polymers. The a_T data points were fitted with an Arrhenius expression since the temperatures studied are more than 100 °C above their glass transition temperatures (−60 to −40 °C).

2.7. Atomic Force Microscopy (AFM). A sample of 1 mg of macromonomer **4** was dissolved in 1 mL of chloroform and was subsequently drop-cast on glass cover slips that were cleaned by sonicating in acetone for 15 min and subsequently dried under vacuum at 40 °C for a few hours. AFM images were recorded at room temperature in air using a Digital Instrument Multimode Nanoscope IV operating in the tapping regime mode using silicon cantilever tips (PPP−NCH-50, 204−497 kHz, 10−130 N/m) with scan rates between 0.5 and 1 Hz. All images are subjected to a first-order plane-fitting procedure to compensate for sample tilt.

3. Results

3.1. Synthesis. To obtain polymer **1**, the amine end groups of the **PCL 2k** intermediate (Scheme 3) were functionalized with UPy moieties. The amine telechelic polymer is not very stable and is thought to decompose via backbiting of the amino end group followed by elimination of a lactam, or by the corresponding intermolecular process. Both reactions result in the loss of the amino end group. Therefore, the intermediate was not isolated but was reacted immediately with activated isocytosine **5**[23] to obtain the directly linked polymers. Macromonomer **2b** was synthesized by reaction of the commercial **PCL 2k** (M_n = 2 kg/mol) with isocyanate-functionalized ureidopyrimidinone (UPy), according to a procedure described previously.[25] Macromonomers **2a** and **2c** were synthesized analogously to **2b**, using polycaprolactones with a molecular weight of 1 and 4 kg/mol, respectively (see the Supporting information).

To obtain macromonomer **3**, modified UPy synthon (**6**; Scheme 4) was synthesized, containing a bulky adamantyl group. This synthon was coupled to the polycaprolactone according to a common procedure.[25]

Macromonomer **4** was obtained by ring opening polymerization of 4-methyl-caprolactone using fumaric acid as a catalyst and hexane diol as initiator (see the Supporting Information) and isocyanate-functionalized ureidopyrimidinone (UPy) was coupled according to a procedure described previously.[25] Molecular weights (M_n) of the products were determined by ^{1}H NMR and by GPC (THF, PS standard) and are listed in Table

Scheme 3. Synthesis of Macromonomer 1 Using Activated Isocytosine 5

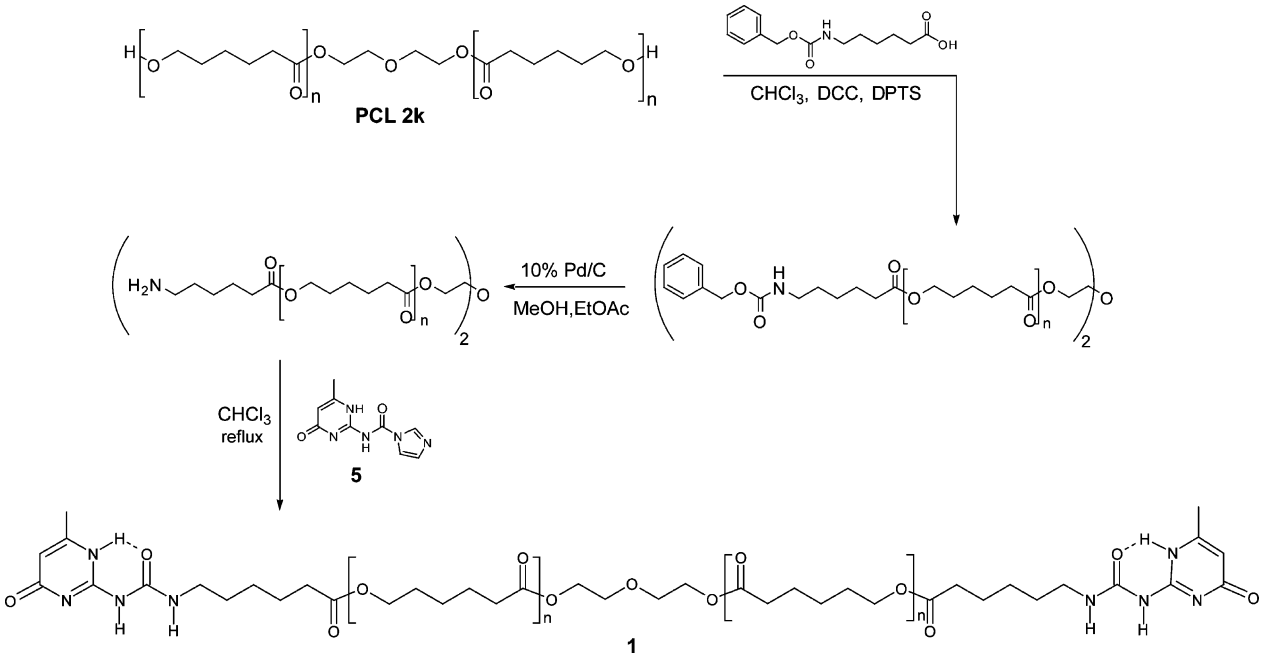

Scheme 4. Synthesis of Adamantyl UPy Synthon 6 Used for the Preparation of Macromonomer 3

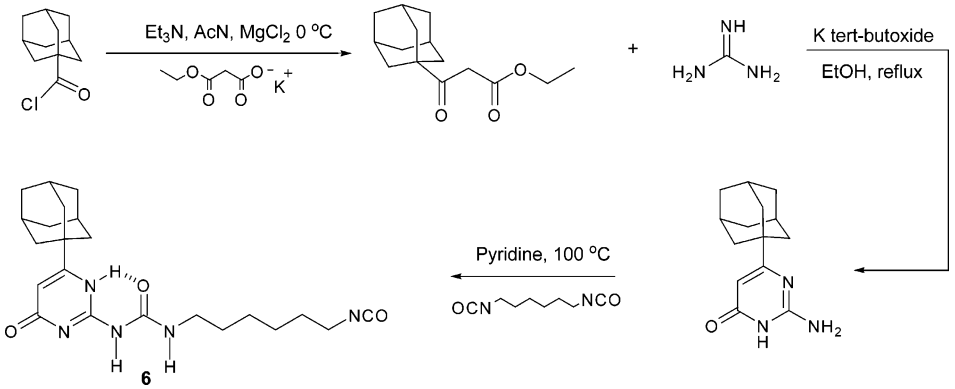

Table 1. Molecular Weights Determined by GPC and HFA, Hydroxyl Groups Per Polymer Chain Determined by ^{19}F NMR Using Peak Integrals at −80.8 ppm and Maximum Supramolecular Degree of Polymerization DP_{max}

polymer	M_n [kg/mol]/ PDI (GPC)[a]	M_n [kg/mol] (^{1}H NMR)	OH groups per polymer chain[b]	DP_{max}[b]
PCL 2k	3.1/1.76	2.0[b]	2	1
1	2.9/1.45	2.5	0.005	4×10^2
2a	1.7/1.29	1.5	0.013	1.5×10^2
2b	3.7/1.68	2.7	0.023	87
2c	7.0/1.49	5.7	0.004	5×10^2
3	4.8/1.88	3.0	0.008	2.5×10^2
4	3.9/1.38	3.4	n.d.	n.d.

[a] Using PS standards. [b] Calculated from ^{19}F NMR.

1. Comparison of the molecular weights of macromolecules **1**−**4** obtained by GPC and ^{1}H NMR (Table 1) shows an overestimation of 25−55%. These values are close to the expected overestimation of 35% reported[51] for molecular weight determination of PCL by GPC using PS standards. Furthermore, the amount of hydroxyl end groups was determined by observation of HFA-adducts in ^{19}F NMR (see below) and from these values the maximum degree of polymerization (DP_{max}) was calculated (Table 1).

3.2. Degree of Functionalization. Purity and hydrogen bond formation between UPy moieties was determined using ^{1}H NMR. In deuterated chloroform, all products showed the characteristic set of three peaks at 13, 11.8, and 10.1 ppm for the intermolecular hydrogen bonds and at 5.8 ppm the intramolecular hydrogen bond was observed for all products. Functionalization of the low molecular weight telechelic polymers led to a very distinct improvement in mechanical properties. Whereas the telechelic **PCL 2k** is a waxy solid, all UPy functionalized products are strong and elastic materials. These differences are attributed to supramolecular chain extension by hydrogen bonding.[18]

^{1}H and ^{13}C NMR do not allow the quantitative determination of very small amounts of unreacted hydroxyl and amine end groups due to insufficient sensitivity of these techniques. A method using hexafluoroacetone (HFA) to determine hydroxyl end groups in polymers has been shown to be successful.[39,52,53] The strength of this method lies in the high sensitivity of ^{19}F NMR, the high ^{19}F chemical shift dispersion, the absence of fluorine in the polymers, and the fact that six fluorine atoms replace a single proton of the hydroxyl group. The product was monitored using ^{19}F NMR, and α,α,α-trifluorotoluene (TFT) was used as internal standard to quantify the concentration of hydroxyl groups. This method was applied to **PCL 2k** and the polymers **2** and **3**, all synthesized starting from hydroxyl end capped polycaprolactones.

Table 2. Thermal Properties from DSC[a]

polymer	T_g [°C]	$T_{m,CL}$ [°C][b]	$T_{m,UPy}$ [°C][b]	ΔH_{total} [J/g]
PCL 2k	−66.3	45, 51		61.6
PCL 80k	−57.0	57.6		46.8
1	−54.2	41.3	49.5	55.6
2a	−39.2	87.6	87.6	18.2
2b	−62.0	40.9	54.5	34.9
2c	−55.5	55.6	55.6	61.2
3	−49.7	44.0		3.9
4	−51.2		39.7	5.8

[a] Data obtained from the second heating run. [b] Assignment of melting peak is based on VTIR (vide infra).

The recorded spectra show the expected signals of TFT (−64.00 ppm), unreacted HFA (−76.31 ppm) and the HFA−water adduct (−83.65 ppm) (see the Supporting Information). The intense peak in both spectra at −80.81 ppm is assigned to the HFA adduct of hydroxyl groups at the end of polycaprolactone (CL−OH) as this peak strongly decreased in intensity after functionalization.

Assuming that the functionality of **PCL 2k** is exactly 2, based on the integrals of CL−OH and TFT, a number average molecular weight of 2.0 kg/mol was calculated, corresponding to the data provided by the supplier. The amount of hydroxyl groups in **2b** based on the residual peak at −80.81 ppm was determined to be 0.024 hydroxyl groups per chain, indicating a high conversion of the UPy functionalization reaction. The other urethane-linked polymers (**2a**, **2c**, and **3**) contain 0.013, 0.004, and 0.008 of unreacted hydroxyl groups per chain, respectively. In the case of polymer **1**, the amount of hydroxyl end groups, formed by intramolecular amidation, was also determined using ^{19}F NMR of the HFA adducts. The intensity of the signal, slightly shifted to −80.83 ppm indicated the presence of 0.005 OH end groups per chain. If it is assumed that the remaining hydroxyl groups are part of unimers functionalized with a single UPy group, these numbers correspond to the fraction of stopper molecules, and the maximum supramolecular degree of polymerization (DP) can be calculated to be >80 in all cases (Table 1). However, in **PCL 2k** as well as in **2a**, **2c**, and **3**, small signals of unknown HFA-adducts are present between −81 and −83 ppm. Since it cannot be excluded that these represent end groups of UPy containing polymers, which also act as chain stoppers, the supramolecular degree of polymerization of the UPy telechelic macromonomers cannot be established with full certainty.

3.3. Thermal Analysis by Differential Scanning Calorimetry. Differential scanning calorimetry (DSC) was used to study thermal properties of the supramolecular polymers as well as the hydroxy telechelic starting material **PCL 2k**. The latter exhibited two melt endotherms at 45 and 51 °C, with a total heat of fusion of 61.6 J/g. Upon functionalization of **PCL 2k** with the different UPy moieties, the glass transition temperature of the supramolecular polymers increased as shown in Table 2. Supramolecular polymer **1** displayed two melting points of 41.3 and 49.5 °C. Two melting peaks, at 40.9 and 54.5 °C, were also observed for supramolecular polymer **2b**. The structural difference between **1** and **2b**, with respectively ester and urethane functionality in close proximity to the UPy moieties, apparently has a minor influence on thermal properties. However, lowering the molecular weight of the polymeric linker between the UPy moieties leads to strong changes in thermal properties; **2a** displayed a higher glass transition (−39.2 °C) and showed a single very broad melting peak, which was shifted to a higher temperature, 87.6 °C. Macromonomer **2c**, with higher molecular weight PCL between the UPy moieties, displayed also different thermal properties: a slightly shifted glass transition temperature compared to **2b** (−55.5 °C) and a single broad melt transition at 55.6 °C. The DSC trace of **3** displays a single melting endotherm at 44.0 °C, with a low melting enthalpy. The low degree of crystallinity of this material suggests that packing of the polymer chains is inhibited by the bulky adamantyl group on the UPy end groups of this polymer. The thermal behavior of macromonomer **4** is similar to that of **3**: one melting peak around 40 °C (39.7 °C) with a low melting enthalpy of 5.8 J/g. The polyester backbone of **4** is amorphous and does not contribute to the crystallinity of the polymer, and therefore, the observed peak originates from the UPy moieties. A crystallization temperature of 20 °C was observed for **PCL 80k**, higher than the crystallization temperatures observed for the polycaprolactone backbones of polymers **1** and **2a**, which are −2.8 and −29.2 °C, respectively. Therefore, it is suggested that the presence of the UPy moieties decreases the crystallization rate of the semicrystalline PCL backbones.

3.4. Variable Temperature Infrared Spectroscopy. Variable temperature attenuated total reflection infrared spectroscopy (VT-IR) is a valuable technique for the assignment of melting of functional groups or polymer parts or to study interactions between polymers after blending,[54−58] since bands often shift or change in intensity when the direct environment of a functional group changes. Coleman[56,59] and others[60,61] have studied polycaprolactone intensively and reported a shift from 1724 cm−1 (crystalline ν_s(C═O)) to 1737 cm^{-1} (amorphous ν_s(C═O)) upon melting. Furthermore, a band at 1293 cm^{-1}, corresponding to the C−O and C−C stretch vibrations in the crystalline phase, also disappeared upon melting. Although the bands of the UPy moiety have not been assigned to specific vibrations,[24,62] a characteristic band has been observed at 1668 cm^{-1}, which shifts to 1661 cm^{-1} upon melting. In the region between 3155 and 3130 cm^{-1}, a band is observed of the intermolecular hydrogen bond of the UPy dimer in the keto tautomeric form.[24] In polymer **2b**, the latter band was observed at all temperatures with little change in intensity. This demonstrates that, at least up to 120 °C, nearly all UPy moieties are present as dimers.

To distinguish between the polyester chain and the UPy moiety, the band at 1293 cm^{-1} was used to evaluate the presence of crystalline polycaprolactone, and the shift from 1668 to 1661 cm^{-1} was used to establish melting of UPy crystallites in the polymer matrix. To disregard differences in molecular weight of the polymer backbone, VT-IR experiments were performed on polymers **1**, **2b**, **3**, and **4**.

Upon heating **2b**, a clear transition between crystalline and amorphous caprolactone was observed by disappearance of the band at 1293 cm^{-1} at 47 °C (Figure 1A), slightly higher than the first observed melting transition in DSC (Table 2). This value of the melting transition of caprolactone corresponds to the values reported in the literature.[60,63,64] At 62 °C, at a somewhat higher temperature than the second melting peak in DSC, a significant shift of the band at 1668 cm^{-1} to 1661 cm^{-1} (Figure 1B) was observed, and therefore, this transition is ascribed to melting of the UPy moieties. Another way of plotting the same data can give a clearer view of melting of the two parts of the polymers. In Figure 1C, the intensity of the bands at 1293 and 1668 cm^{-1} of **2b** are plotted against temperature to clearly show the transitions occurring for the two melting processes. The signals corresponding to the melting of the UPy moiety and of caprolactone occur closely to each other for **1**, as was also observed in DSC (Figure 1D, Table 2). A closer look reveals melting of the caprolactone part at 51 °C and the UPy melts at

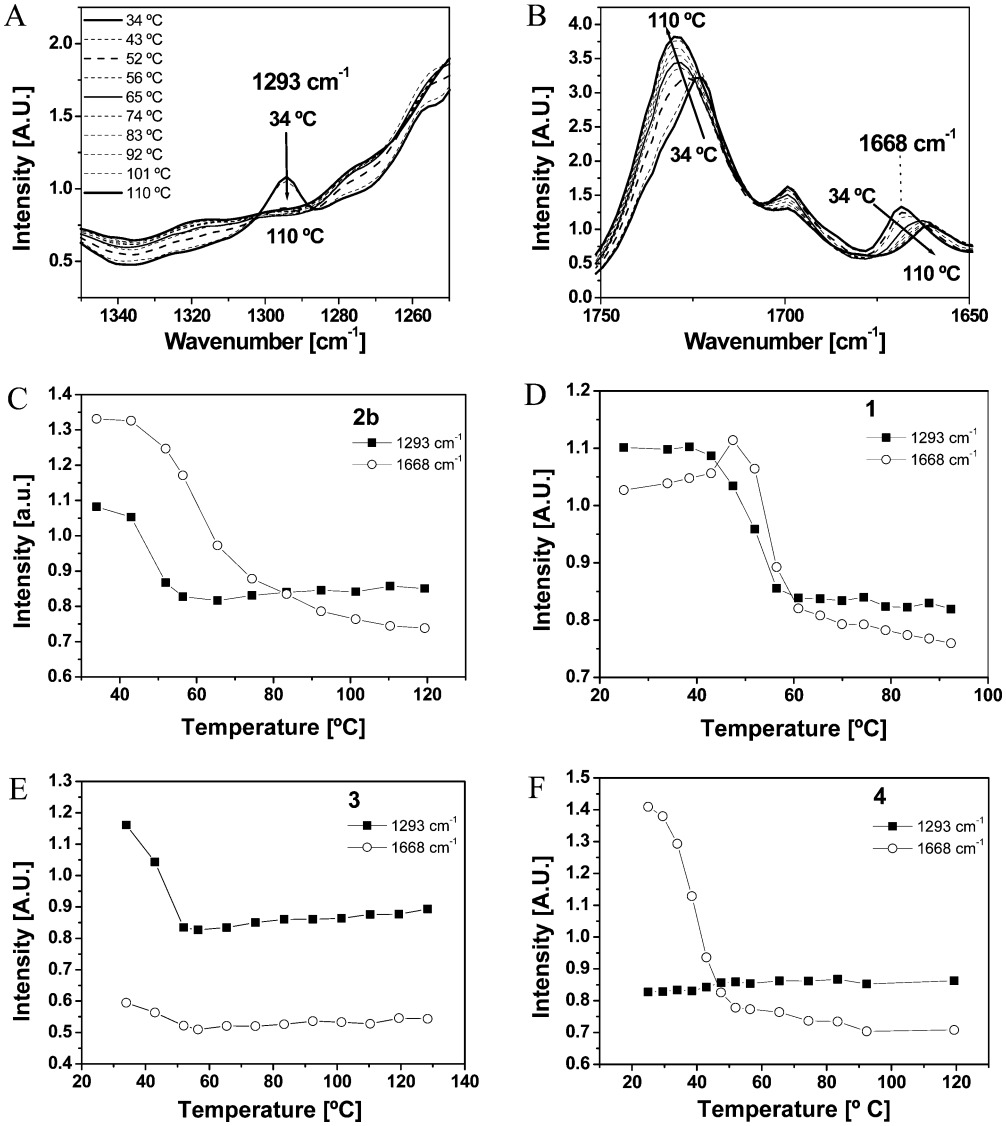

Figure 1. VT-IR of (A) intensity vs wavenumber for the CL region of **2b**; (B) intensity vs wavenumber for the UPy region of **2b**; (C) intensity vs temperature for **2b**; (D) intensity vs temperature for **1**; (E) intensity vs temperature for **3**; (F) intensity vs temperature for **4**.

a temperature of 54 °C. These values differ from the values observed in DSC, which is probably due to the fact that the melting of the two parts occurs simultaneously and influence each other.

In compound **3** (Figure 1E), the intensity of the band of the UPy dimer at 1668 cm^{-1} was nearly constant, indicating that melting of the UPy moieties is not occurring. At 44 °C, a clear transition in the intensity of the signal at 1293 cm^{-1} is observed, which corresponds nicely to the value of the melting peak observed in DSC and is hereby assigned to melting of caprolactone. Opposite behavior is observed for macromonomer **4** (Figure 1F), and as expected, a constant value for the intensity at 1293 cm^{-1} is observed, indicating the absence of a melting transition for methylcaprolactone. The change in intensity for the signal at 1668 cm^{-1} is observed at 40 °C, corresponding to the value found in DSC, and this melting transition is assigned to melting of the UPy moiety.

3.5. Atomic Force Microscopy. The UPy segments of telechelic PEB have been shown with atomic force microscopy (AFM) to crystallize in very long fibrils.[27] Similar fibers were observed by Wilkes et al. when examining segmented polyurethaneurea copolymers with the same[65,66] and other soft segments[67] by AFM. The observed fibers are attributed to stacking via hydrogen bonds between the urethanes and ureas present in the copolymers. Visualization of the proposed UPy stacks in urethane coupled UPy polycaprolactones **2** using AFM is hindered by the high crystallinity of caprolactone, which will result in images displaying mainly crystalline plates of caprolactone.[47] Measuring AFM on **2b** at a temperature above the melting temperature of caprolactone is not possible as the molten caprolactone becomes very sticky and the AFM tip cannot slide over the polymer film. Therefore, macromonomer **4** (M_n = 3.9 kg/mol) containing an amorphous poly-4-methyl-caprolactone backbone was studied with AFM. This material displayed a single melting temperature with a low melting enthalpy, attributed to melting of the UPy crystallites (vide supra). In the AFM image (Figure 2) of a drop cast film of **4**, fibers are clearly visible. Because the polymer backbone is amorphous in **4**, the fibers originate from crystallization of the UPy moieties, which melt at 40 °C.

3.6. Oscillatory Shear Experiments. The improvement in mechanical properties and the change in thermal properties show that functionalization of polymers with UPy end groups has an enormous impact on their properties. Oscillatory shear experiments in the linear viscoelastic regime were performed to get insight in the mechanism of the formation of higher molecular

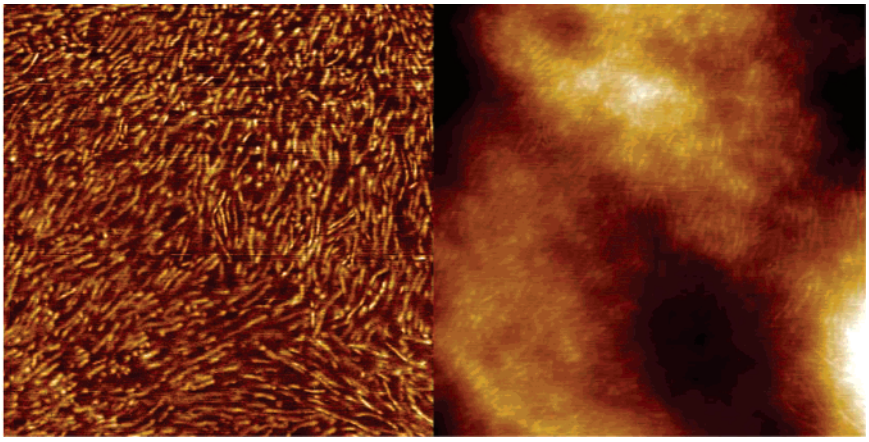

Figure 2. AFM phase image (left) and height image (right) of **4** at room temperature. Images at 1 μm scan size, Z range is 15 nm and $\Delta\varphi$ is 7°.

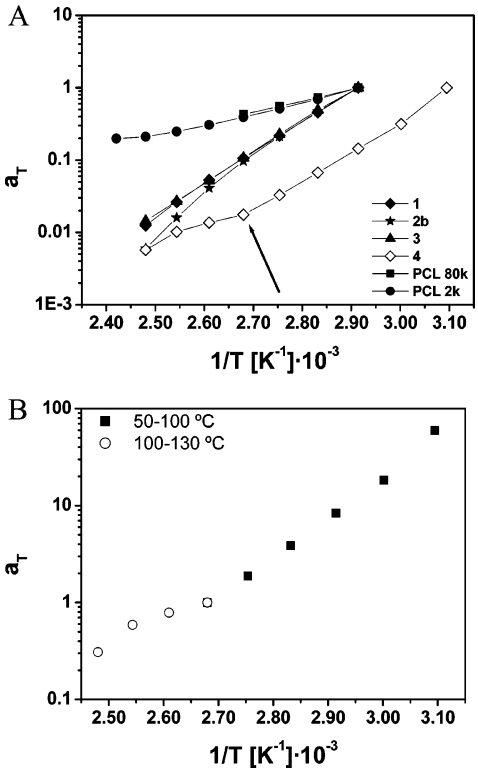

Figure 3. Horizontal shift factors a_T vs inverse temperature $1/T$ of (A) polymers **1**−**4** and (B) polymer **4** in which 100 °C is used as T_{ref} for both temperature regimes.

weight species and identification of the rheological relaxation processes. All experiments were performed in the melt between 70 and 130 °C, above the melting temperatures (Table 2) and well below the temperature (∼150 °C) at which ureidopyrimidinone units degrade thermally.

To enable comparison of the supramolecular polymers with covalent PCL, rheological properties of **PCL 2k** and **PCL 80k** were measured too. For the low molecular weight **PCL 2k** a very low, frequency independent complex viscosity (∼1 Pa•s at 70 °C) was observed, characteristic for low molecular weight polymers.

The horizontal shift factors a_T, used to create rheological master curves for all polymers are shown in Figure 3A. The slopes for **PCL 2k** and **PCL 80k** are similar in value (1.5×10^3 and 1.4×10^3, respectively), indicating a similar temperature dependence of the polymers. The slopes of the curves in Figure 3A (listed in Table 3) for the supramolecular polymers ($3.5-5.1 \times 10^3$ K) are significantly higher than for the covalent polycaprolactones. The high values for the supramolecular polymers indicate that their rheology is much more temperature dependent than for the covalent ones. Surprisingly, the slope in the plot of polymer **4** changes strongly at a temperature of 100 °C as can be seen in Figure 3B, indicating a transition of unknown origin.

Table 3. Slopes of Horizontal Shift Factors (a_T) vs Temperature and Activation Energies (E_a) from Arrhenius Plot

polymer	slope [K]	E_a [kJ/mol]
PCL 2k	1.5×10^3	30.0
PCL 80k	1.4×10^3	28.0
1	4.3×10^3	83.3
2b	5.1×10^3	97.3
3	4.3×10^3	82.1
4	4.2×10^3 (50−100 °C)	79.8
	2.4×10^3 (100−130 °C)	45.4

From the Arrhenius plot (Figure 3A,B), activation energies can be calculated using eq 1

$$\log a_T = C(E_a) + 0.4343\frac{E_a}{RT} \quad (1)$$

The values of the calculated activation energies are also listed in Table 3. For conventional polycaprolactones a value of 40 kJ/mol is reported in literature.[68] The values for the polycaprolactons are somewhat lower, whereas those of the supramolecular polymers are considerably higher. The activation energy found for the low-temperature regime of polymer **4** (50−100 °C) corresponds to the values obtained for the other supramolecular polymers, whereas in the high-temperature regime (100−130 °C), a value closer to the values of the unfunctionalized polycaprolactones is observed.

Master curves of G' and G'' for **PCL 80k** using the WLF time temperature superposition principle (TTS)[69] and a reference temperature of 70 °C are shown in Figure 4A. This polymer shows the normal viscoelastic behavior as expected, with slopes of 2 and 1 for G' and G'' in the terminal (flow) regime and a plateau modulus of 2×10^5 Pa. Polydispersity and Rouse-like relaxation modes lead to curvature in the plot of G' in the frequency range just below the plateau. It is not possible to measure the rubberlike plateau zone and the transition to glassy region of our polymers and supramolecular polymers, because for that purpose much higher frequencies are needed (e.g., forced vibrations in resonance (10^5 rad/s) or even wave propagation (up to 2×10^{10} rad/s)[70]). For the other method (TTS) we would have to make use of temperatures lower than 70 °C in order to increase the frequencies of the master curve. However, this is

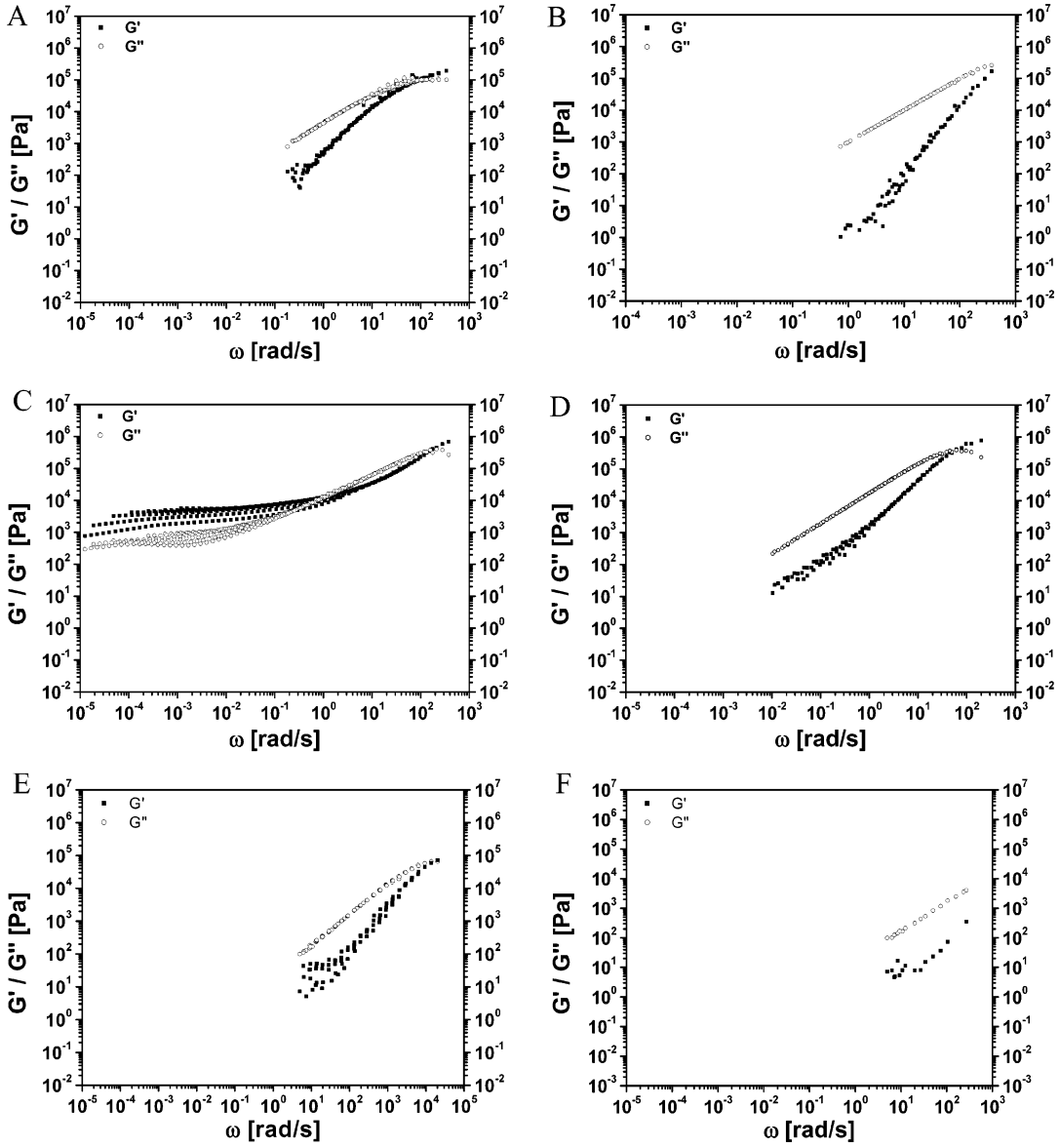

Figure 4. Master curves of (A) **PCL 80k**, (B) **1**, (C) **2b**, (D) **3**, (E) **4**, 50−100 °C, T_{ref} = 100 °C, and (F) **4** 100−130 °C, T_{ref} = 100 °C. Storage modulus (G'; filled squares) and loss modulus (G''; open circles) vs angular frequency of oscillation.

not possible because the melting temperatures of the polymers used are close to 70 °C.

Although the molecular weight of the monomer of supramolecular polymer **1** is only slightly higher (2.9 kg/mol) than of its precursor (2.0 kg/mol), high values of 10^5-10^6 Pa were measured for the plateau of the storage modulus (Figure 4B), similar to the values reached for **PCL 80k**.

Like in **PCL 80k**, a crossover for G' and G'' is observed in Figure 4B, but here the plot shows almost ideal Maxwell behavior with slopes of 2.0 (G') and 1.0 (G''), and little curvature up to the crossing point of the curves where Rouse like modes start to dominate the relaxation behavior. Because the high-frequency part is not accessible, a Cole−Cole plot (see the Supporting Information) cannot be used to demonstrate Maxwellian behavior in the rubber plateau. However, behavior of **1** in the frequency range up to the rubber plateau can be described by a single Maxwell element with a relaxation time of 1.6 ms.

The apparent scattering of the storage modulus observed in the low-frequency range of the supramolecular polymers, and in particular of macromonomer **4,** is in fact a systematic change with temperature. We attribute this systematic deviation to the presence of a very fragile, low modulus physical network that does not obey the normal WLF time temperature superposition. This becomes very clear in the rheology of **2b** (Figure 4C) where a plateau zone is present with an equilibrium shear modulus, G_e, which decreases from 5700 Pa at 70 °C to 2050 Pa at 130 °C. The presence of such a network is not clear in **1** and **3**: here physical cross-links may be present but not enough to form a physical network (less than one cross-link per weight average supramolecular polymer if the functionality of the cross-links is 4). Because of the height of the loss moduli, they will be hardly affected by the formation of the network in the range of frequencies measured. For that reason, the TTS can still be applied on the measurements of the loss moduli, even if physical cross-links are present.

The single structural difference between macromonomers **2b** and **1** is the presence of a urethane linkage in close proximity to the UPy end group instead of an ester. Nevertheless, the master curves of compound **2b** (Figure 4C) differ drastically from that of **1**.

Oscillatory shear experiments on macromonomers **2a** and **2c** show that the presence of the plateau at low frequencies is dependent on the density of functional end groups (Figure 5). The master plot (Figure 5A) of the shorter macromonomer **2a**

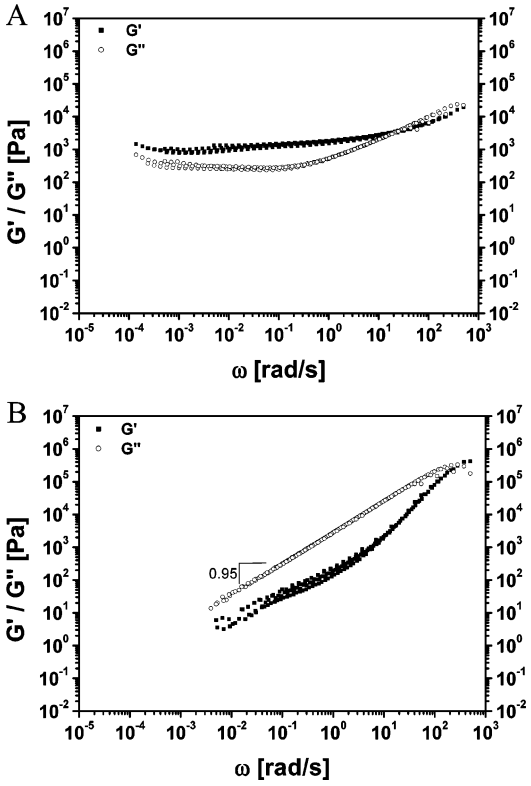

Figure 5. Master curves of (A) **2a** and (B) **2c**. Storage modulus (G'; filled squares) and loss modulus (G''; open circles) vs angular frequency of oscillation. Reference temperature for the time temperature shifts was 100 and 70 °C, respectively.

(M_n = 1 kg/mol) is similar to the master curve of **2b**. Concurrent with the increased concentration of end groups in this material, the formation of the reversible network is enhanced and the observed plateau in G' extends to higher frequencies than for **2b**. The origin of this plateau is believed to be similar for both polymers as the value at low frequencies for the loss modulus is similar (~5 kPa) in both cases. In contrast to **2a** and **2b**, no plateau in G' was observed for **2c**, which has a M_n of 7 kg/mol. Although, the slope of G'' is approximately 1, the terminal regime was not reached for **2c** as the slope of G' is smaller than 2.

The Arrhenius plot of macromonomer **4** which has an amorphous poly-4-methyl-caprolactone backbone (Figure 3B) shows a change in slope around 100 °C. Therefore, two master plots were created: one for the temperature range below 100 °C (Figure 4E) and one for the range from 100−130 °C (Figure 4F). The transition temperature (100 °C) was used as reference temperature in each of these curves. Below 100 °C, the terminal regime is not reached, whereas fanning out of the curves for G' indicates failure of TTS. Although the number of data points in the temperature range of 100−130 °C is limited, the master curve in Figure 4F for the higher temperature range suggests that also here the terminal regime is not reached. Both the origin of the intensive scattering in Figure 4E compared to the other master curves and the nonlinearity of the Arrhenius plot remain unknown.

In order to further investigate the structural requirements for the presence of a low-frequency plateau in the storage modulus, derivative **3** was investigated, which features an adamantyl substituent on the UPy moieties in addition to the urethane groups that are thought to be necessary for the formation of physical cross-links. The adamantyl groups are quite bulky and are expected to hinder stacking of UPy dimers. The rheological

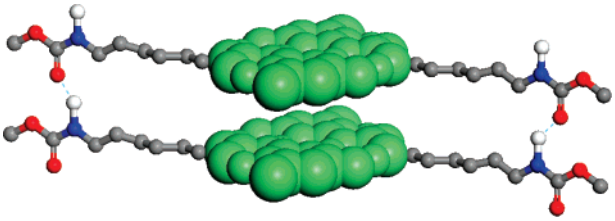

Figure 6. Schematic representation of UPy dimer stacking in **2**. UPy dimers are indicated in green, urethane groups are color-labeled by atom type.

master curves of this compound lack a distinct plateau, although a slight curvature of G' is observed in the low-frequency regime (Figure 4D). Application of TTS on the separate temperature-frequency curves of macromonomer **3** was performed although in the low-frequency regime the TTS is less successful than for the high-frequency regimes. However, failure of TTS to such an extent as seen for **2b** was not observed for **3**, indicating simpler rheological behavior, although physical cross-links are certainly present, but not enough to form a physical network.

In the high-frequency regime a value of 6.6×10^5 Pa is found for the storage modulus of macromonomer **3**, which is somewhat higher than the value found for **1** (1.7×10^5 Pa) but close to the value found for the storage modulus of **2b** (6.1×10^5 Pa). When Maxwell behavior is assumed, the terminal relaxation time can be derived from the crossover frequency, where G' and G'' are equal. For **3**, this leads to a relaxation time of 18.3 ms, close to the terminal relaxation time of **PCL 80k**, which is 14.6 ms.

4. Discussion

In this work, the role of stacking and additional hydrogen bonding interactions in UPy functionalized polycaprolactones are investigated. Thermal properties and surface properties were investigated in the semicrystalline state of the polymers, whereas rheology was measured in the melt. In the telechelic polycaprolactones, microphase separation and crystallization of the UPy groups was observed with VTIR. The melting point of the UPy containing blocks was highest when urethane groups were present, except for polymer **3**, where the bulky adamantyl groups completely prevent crystallization. Previously, we have shown that additional hydrogen bonding interactions between urea or urethane groups close to the UPy groups give rise to fiber-like features in supramolecular polymers based on poly(ethylene butylene)s,[18,27] in trimethylene carbonates,[71] and also in polycaprolactones.[47] In polymer **4**, fibers could indeed be observed with AFM.

Urethane groups are hydrogen bond donors as well as acceptors.[54,72] We propose that in the fibers UPy dimers are stacked, and urethane hydrogen bonding occurs roughly parallel to the stacking direction. A cartoon of two layers in such a stack is shown in Figure 6. Above their melting points, all UPy functionalized PCL derivatives show a remarkable enhancement of rheological properties compared to their hydroxytelechelic precursors, as was previously observed for other polymers.[18,27] Furthermore, it was already suggested from melt viscosity profiles of UPy functionalized poly(styrene) and poly(isoprene) polymers that aggregates of UPy end groups might be present in the melt.[73] Yet, striking differences in behavior between the PCL's are observed.

The rheological behavior of **1** confirms the conclusion, already evident from its physical appearance, that it is a supramolecular polymer in which multiple units bind to each other via hydrogen bonds. The assumed maxwellian behavior

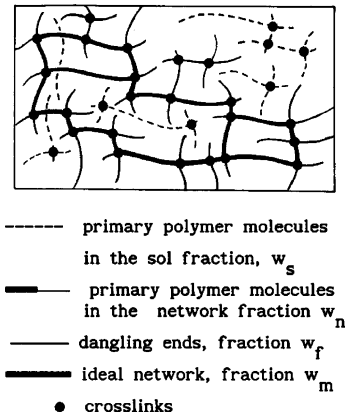

Figure 7. Schematic representation of a nonideal gel network.

of **1** is in agreement with Cates' predictions for linear supramolecular (or "reversible") polymers with fast breaking dynamics compared to the reptation time scale. Cates[28,31] predicts that the behavior of such polymers is characterized by a single relaxation time τ, which is the geometrical mean of the reptation time, τ_{rep}, and the average time, τ_{break}, before a break occurs anywhere along the polymer chain $\tau = (\tau_{rep}\tau_{break})^{1/2}$. As a result, the rheology of such polymers is like that for monodisperse covalent polymers even though a statistical (Flory) molecular weight distribution with $M_w/M_n = 2$ is expected. In contrast to this, a supramolecular polymer with $\tau_{break} > \tau_{rep}$ would display the rheology of a polydisperse polymer with significant curvature of G' and G'' below the crossing point of the curves. From the rheological behavior of **1** and the absence of a low-frequency plateau for G', it can therefore be concluded that the UPy end groups of this polymer associate in a highly directional fashion to give linear supramolecular chains with a lifetime which is significantly shorter than 1.6 ms at 70 °C. The lifetime of the individual dimerized UPy units is expected to be longer (proportionally to the supramolecular DP, which may be up to 400 for **1**), since dissociation of any of the UPy dimers along the chain will result in scission of the supramolecular polymer. When the DP of the materials is known, it is possible to calculate the lifetime of a single UPy dimer in the melt, thus establishing a direct relationship between molecular and rheological parameters. Unfortunately, the actual DP of **1** cannot be given.

A molecular interpretation of the remarkable differences in rheology between **1** and **2b** (viz. the presence of a plateau in G' in **2b**) should be based on the presence of urethane groups in the latter. We propose that in UPy telechelic polymers **2a**, **2b**, **2c**, **4**, and to some extent in **3**, short stacks of laterally aggregated UPy dimers remain present well above the melting point of these moieties observed in DSC and with VT-IR, giving rise to a physical network. In the case of compound **2b**, the physical network persists at a temperature of 130 °C, more than 70 °C above the melting point. We have analyzed this network with the Flory−Stockmayer theory for tetrafunctional cross-linking of monodisperse high molecular weight polymers, extended by one of the authors for cross-links of any functionality and for polydisperse polymers.[74−81] Physical networks are in general far from ideal (Figure 7).[82]

Many polymer molecules are present which are not bound to the network (sol fraction w_s). Moreover many polymer molecules, or small parts of them, form dangling or free ends (fraction w_f) which also do not contribute to the rubber shear modulus G_e. Only the ideal part of the network (fraction w_m) contributes to the rubber shear modulus. The network fraction is equal to $w_n = w_f + w_m$ and $w_s + w_f + w_m = w_s + w_n = 1$.

Table 4. Temperature-dependent Crosslink Index γ_w for Polymer 2b, Calculated for Crosslink Functionalities 4 and 20

T [°C]	G_e [Pa]	γ_w ($f = 4$)	γ_w ($f = 20$)
70	5709	3.39	1.48
80	5065	3.23	1.38
90	4636	3.12	1.31
100	4120	2.99	1.23
110	3834	2.91	1.18
120	2978	2.67	1.05
130	2049	2.37	0.86

The extended Flory−Stockmayer theory can be used to calculate the cross-link index γ_w, i.e., the average number of cross-links per weight average primary polymer (in our case per primary supramolecular polymer), from G_e, i.e., the equilibrium shear modulus, for a known cross-link functionality and a Schultz−Flory molecular weight distribution with $M_w/M_n = 2$. For polymer **2a**, γ_w was calculated at a number of temperatures, using a value of 239 kg/mol for the maximum attainable M_n estimated from end group titration. These values were calculated for stacks of two dimers (cross-link functionality $f = 4$) and for stacks of 10 dimers ($f = 20$; cross-link functionality f means that f chains leave the cross-link; Table 4).

If we assume that the cross-links formed by the sections for the polymers that contain the dimerized UPy moieties and urethane groups and that these cross-links are subject to a thermoreversible equilibrium, we find a relationship between the cross-linking index and the absolute temperature in the following way:

$$K_{eq} = \frac{[\text{crosslinks}]}{[\text{UPydimers}]^{f/2}} = K^0 \exp\left(\frac{-\Delta H}{RT}\right) \tag{2}$$

where ΔH is the enthalpy of equilibrium.

For the concentration of cross-links, we have

$$[\text{crosslinks}] = \frac{2}{f}\gamma_w \frac{c}{M_w} \tag{3}$$

Because the concentration of UPy dimers is practically constant, this results in

$$K_{eq} = C\gamma_w \frac{c}{2M_w} = K^0 \exp\left(\frac{-\Delta H}{RT}\right) \tag{4}$$

so that

$$\gamma_w \propto \exp\left(\frac{-\Delta H}{RT}\right) \tag{5}$$

Hence upon plotting ln γ_w vs $1/T$, a straight line should be obtained with slope equal to $-\Delta H/R$ (Figure 8).

From the slope of the straight line fitted through the points for $f = 4$, a value of $\Delta H = -6.4$ kJ/mol was derived, whereas for $f = 20$, $\Delta H = -9.3$ kJ/mol was found. The interaction energy of a dimeric stack ($f = 4$) has a value of −6.4 kJ/mol per pair. In the case of the decameric stack ($f = 20$), a interaction energy of (−9.3/9 =) −1.03 kJ/mol per pair is calculated. Furthermore, the rather low (absolute) value of −6.4 kJ/mol is of the order of the interaction energy between benzene rings and also of the order of the interaction energy between mesogenic groups in discotic side chain liquid crystalline polymers.[83,84] Hence, it is not unreasonable to attribute the cross-link formation to the interaction between UPy dimers, which self-assemble into small (dimeric) stacks. Small aggregates of poly(THF) functionalized with modified adenine were shown to be responsible, in combination with phase separation, for the

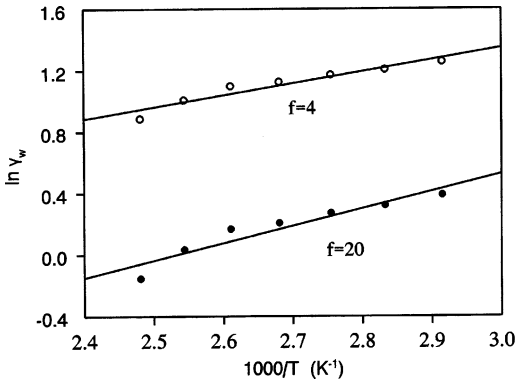

Figure 8. Weight average cross-linking index, γ_w, for polymer **2b** plotted logarithmically vs reciprocal temperature (K^{-1}) for $f = 4$ and 20.

formation of a temperature-dependent physical network with a relatively high plateau modulus.[45] The present work shows that relatively weak interactions (single hydrogen bonds) are also able to create a physical network with significant moduli in supramolecular polymers when the main chain is concatenated via strong quadruple hydrogen bonds.

Aggregation is also concentration dependent, since it is suppressed by lowering the UPy group concentration in higher molecular weight material **2c**. The stacking of dimerized UPy groups into stacks above the melting point is a process preceding the crystallization observed in DSC, which is a true phase transition. We tentatively propose that the physical cross-links in the melt form nuclei for crystallization at lower temperatures. Future studies will be directed to understanding the nature of the aggregation process in the melt, in particular whether the stacking is an isodesmic or a nucleated process.[85]

In the absence of lateral interactions, like in polymer **1**, the rheological behavior is much simpler. Further investigation to get insight in the relation between UPy dimer lifetime and melt rheology will therefore be focused on polymer **1** and analogs in which the molecular weight is controlled by the presence of monofunctional stopper molecules.

5. Conclusion

The results presented here show that the melt rheology of polar UPy telechelic polymers is strongly influenced by the capability of UPy dimers to further aggregate by means of stacking. We had previously shown that the physical cross-linking, which is the result of aggregation, strongly improves the mechanical properties of an apolar UPy-telechelic polymer. With the present work, we have explored the consequences of UPy stacking for melt processing of polar polymers, and we have shown how end group aggregation in these polymers can be controlled by minor structural modifications.

Acknowledgment. We thank Michiel Beeren for synthesis of macromonomer **2c**, Jorg Roosma for the synthesis of macromonomer **4**, and Dr. Oren Scherman and Prof. W. J. Feast for their help with the HFA procedure. We thank Eva Wisse for measuring the AFM images of macromonomer **4** and Prof E.W. Meijer for useful discussions. Financial support (D.J.M-.v.B.) from NanoImpuls/NanoNed, the nanotechnology program of the Dutch Ministry of Economic Affairs, is gratefully acknowledged.

Supporting Information Available: Synthesis and characterization (NMR, DSC, and GPC) of macromonomers **1**−**4**. ^{19}F NMR spectra. Master curve of **PCL 2k** and complex viscosities of **PCL 2k**, **PCL 80k**, **1**, **2a**, **2b**, **2c**, and **3** vs frequency of oscillation. Equations for calculation of crosslinking index from equilibrium shear modulus. This material is available free of charge via the Internet at http://pubs.acs.org.

References and Notes

(1) Brunsveld, L.; Folmer, B. J. B.; Meijer, E. W.; Sijbesma, R. P. *Chem. Rev.* **2001**, *101* (12), 4071−4097.
(2) Moore, J. S. *Curr. Opin. Colloid Interface Sci.* **1999**, *4*, 108−116.
(3) Armstrong, G.; Buggy, M. *J. Mater. Sci.* **2005**, *40*, 547−559.
(4) Ciferri, A. *Supramolecular Polymers*, 2nd ed.; CRC Press: Boca Raton, FL, 2005.
(5) Bosman, A. W.; Sijbesma, R. P.; Meijer, E. W. *Mater. Today* **2004**, *7* (4), 34−39.
(6) Lehn, J. M. *Makromol. Chem., Macromol. Symp.* **1993**, *69*, (4th European Polymer Federation Symposium on Polymeric Materials, 1992), 1−17.
(7) Fouquey, C.; Lehn, J. M.; Levelut, A. M. *Adv. Mater.* **1990**, *2* (5), 254−257.
(8) Murray, T. J.; Zimmerman, S. C. *J. Am. Chem. Soc.* **1992**, *114*, 4010−4011.
(9) Corbin, P. S.; Zimmerman, S. C. *J. Am. Chem. Soc.* **1998**, *120* (37), 9710−9711.
(10) Beijer, F. H.; Sijbesma, R. P.; Kooijman, H.; Spek, A. L.; Meijer, E. W. *J. Am. Chem. Soc.* **1998**, *120* (27), 6761−6769.
(11) Kolomiets, E.; Buhler, E.; Candau, S. J.; Lehn, J.-M. *Macromolecules* **2006**, *39* (3), 1173−1181.
(12) Corbin, P. S.; Zimmerman, S. C.; Thiessen, P. A.; Hawryluk, N. A.; Murray, T. J. *J. Am. Chem. Soc.* **2001**, *123* (43), 10475−10488.
(13) Li, M.; Yamato, K.; Ferguson, J. S.; Bong, B. *J. Am. Chem. Soc.* **2006**, *128* (39), 12628−12629.
(14) Zirbs, R.; Kienberger, F.; Hinterdorfer, P.; Binder, W. H. *Langmuir* **2005**, *18*, 8414−8421.
(15) Binder, W. H.; Kluger, C.; Josipovic, M.; Straif, C. J.; Friedbacher, G. *Macromolecules* **2006**, *39*, 8092−8101.
(16) Binder, W. H.; Bernstorff, S.; Kluger, C.; Petraru, L.; Kunz, M. J. *Adv. Mater.* **2005**, *17*, 2824−2828.
(17) Beijer, F. H.; Kooijman, H.; Spek, A. L.; Sijbesma, R. P.; Meijer, E. W. *Angew. Chem., Int. Ed.* **1998**, *37* (1/2), 75−78.
(18) Folmer, B. J. B.; Sijbesma, R. P.; Versteegen, R. M.; van der Rijt, J. A. J.; Meijer, E. W. *Adv. Mater.* **2000**, *12* (12), 874−878.
(19) Park, T.; Zimmerman, S. C. *J. Am. Chem. Soc.* **2006**, *128*, 13986−13987.
(20) Park, T.; Zimmerman, S. C. *J. Am. Chem. Soc.* **2006**, *128*, 14236−14237.
(21) McKee, M. G.; Elkins, C. L.; Park, T.; Long, T. E. *Macromolecules* **2005**, *38*, 6015−6023.
(22) ten Cate, A. T.; Sijbesma, R. P. *Macromol. Rapid Commun.* **2002**, *23*, (18), 1094−1112.
(23) Keizer, H. M.; Sijbesma, R. P.; Meijer, E. W. *Eur. J. Org. Chem.* **2004**, *35* (41), 2553−2555.
(24) Söntjens, S. H. M. Ph.D. Thesis, Technische Universiteit Eindhoven: Eindhoven, The Netherlands, 2002.
(25) Dankers, P. Y. W.; Harmsen, M. C.; Brouwer, L. A.; van Luyn, M. J. A.; Meijer, E. W. *Nat. Mater.* **2005**, *4* (7), 568−574.
(26) Dankers, P. Y. W.; van Leeuwen, E. N. M.; van Gemert, G. M. L.; Spiering, A. J. H.; Harmsen, M. C.; Brouwer, L. A.; Janssen, H. M.; Bosman, A. W.; van Luyn, M. J. A.; Meijer, E. W. *Biomaterials* **2006**, *27*, 5490−5501.
(27) Kautz, H.; van Beek, D. J. M.; Sijbesma, R. P.; Meijer, E. W. *Macromolecules* **2006**, *39* (13), 4265−4267.
(28) Cates, M. E. *Macromolecules* **1987**, *20* (9), 2289−2296.
(29) Lortie, F.; Boileau, S.; Bouteiller, L.; Chassenieux, C.; Lauprêtre, F. *Macromolecules* **2005**, *38* (12), 5283−5287.
(30) Cates, M. E.; Candau, S. J. *J. Phys.: Condens Matter* **1990**, *2*, 6869−6892.
(31) Cates, M. E. *J. Phys. Chem.* **1990**, *94* (1), 371−375.
(32) Hilger, C.; Stadler, R.; de Lucca Fretas, L. L. *Polymer* **1990**, *31*, 818−823.
(33) Seidel, U.; Stadler, R.; Fuller, G. G. *Macromolecules* **1994**, *27* (8), 2066−2072.
(34) Müller, M., Seidel, U., Stadler, R. *Polymer* **1995**, *36* (16), 3143−3150.
(35) Leibler, L.; Rubinstein, M.; Colby, R. H. *Macromolecules* **1991**, *24* (16), 4701−4707.
(36) Jongschaap, R. J. J.; Wientjes, R. H. W.; Duits, M. H. G.; Mellema, J. *Macromolecules* **2001**, *34* (4), 1031−1038.
(37) Rubinstein, M.; Semenov, A. N. *Macromolecules* **2001**, *34* (4), 1058−1068.
(38) Keizer, H. M., Sijbesma, R. P., Meijer, E. W. *Eur. J. Org. Chem.* **2004**, 2533−2555.

(39) Keizer, H. M.; van Kessel, R.; Sijbesma, R. P.; Meijer, E. W. *Polymer* **2003**, *44* (19), 5505−5511.
(40) Elkins, C. L.; Park, T.; McKee, M. G.; Long, T. E. *J. Polym. Sci., Part A: Polym. Chem.* **2005**, *43*, 4618−4631.
(41) Yamauchi, K.; Kanomata, A.; Inoue, T.; Long, T. E. *Macromolecules* **2004**, *37* (10), 3519−3522.
(42) Yount, W. C.; Loveless, D. M.; Craig, S. L. *Angew. Chem., Int. Ed.* **2005**, *44*, 2746−2748.
(43) Yount, W. C.; Loveless, D. M.; Craig, S. L. *J. Am. Chem. Soc.* **2005**, *127*, 14488−14496.
(44) Loveless, D. M.; Jeon, S. L.; Craig, S. L. *J. Mater. Chem.* **2007**, *17*, 56−61.
(45) Sivakova, S; Bohnsack, D. A.; Mackay, M. E.; Suwanmala, P.; Rowan, S. J. *J. Am. Chem. Soc.* **2005**, *127*, 18202−18211.
(46) Wisse, E; Spiering, A. J. H.; van Leeuwen, E. N. M.; Renken, R. A. E.; Dankers, P. Y. W.; Brouwer, L. A.; van Luyn, M. J. A.; Harmsen, M. C.; Sommerdijk, N. A. J. M.; Meijer, E. W. *Biomacromolecules* **2006**, *7* (12), 3385−3395.
(47) Dankers, P. Y. W. Ph.D. Thesis, Technische Universiteit Eindhoven: Eindhoven, The Netherlands, 2006.
(48) Trinkle, S.; Hoffmann, B.; Kricheldorf, H. R.; Friedrich, C. *Macromol. Chem. Phys.* **2001**, *202* (6), 814−823.
(49) Stridsberg, K. M.; Ryner, M.; Albertsson, A.-C., *Controlled-Ring-Opening Polymerization: Polymers with designed Macromolecular Architecture*; Springer: Berlin, 2002; Vol. 157/2001, pp 41−65.
(50) Peeters, J.; Palmans, A. R. A.; Veld, M.; Scheijen, F.; Heise, A.; Meijer, E. W. *Biomacromolecules* **2004**, *5* (5), 1862−1868.
(51) Ramkumar, D. H. S.; Bhattacharya, M. *Polym. Eng. Sci.* **1998**, *38* (9) 1426−1435.
(52) Ronda, J. C.; Serra, A.; Mantecón, A.; Cádiz, V. *Macromol. Chem. Phys.* **1994**, *195*, 3459−3468.
(53) Ho, F. F.-L. *Anal. Chem.* **1973**, *45* (3), 603−605.
(54) Coleman, M. M.; Lee, K. H.; Skrovanek, D. J.; Painter, P. C. *Macromolecules* **1986**, *19* (8), 2149−2157.
(55) Vermeesch, I. M.; Groeninckx, G.; Coleman, M. M. *Macromolecules* **1993**, *26* (24), 6643−6649.
(56) Coleman, M. M.; Moskala, E. J. *Polymer* **1983**, *24*, 251−257.
(57) Mattia, J.; Painter, P. *Macromolecules* **2007**, *40* (5), 1546−1554.
(58) Painter, P.; Sobkowiak, M.; Park, Y. *Macromolecules* **2007**, *40* (5), 1730−1737.
(59) Coleman, M. M.; Zarian, J. *J. Polym. Sci., Polym. Phys. Ed.* **1979**, *17*, 837−850.
(60) Jutier, J.-J.; Lemieux, E.; Prud'homme, R. E. *J. Polym. Sci., Part B: Polym. Phys.* **1988**, *26*, 1313−1329.
(61) Elzein, T.; Nasser-Eddine, M.; Delaite, C.; Bistac, S.; Dumas, P. *J. Colloid Interface Sci.* **2004**, *273* (2), 381−387.
(62) Beijer, F. H.; Ph.D. Thesis, Technische Universiteit Eindhoven, Eindhoven, The Netherlands, 1998.
(63) Kuo, S. W.; Huang, C. F.; Chang, F. C. *J. Polym. Sci., Part B: Polym. Phys.* **2001**, *39*, 1348−1359.
(64) Crescenzi, V.; Manzini, G.; Calzolari, G.; Borri, C. *Eur. Polym. J.* **1972**, *8* (3), 449−463.
(65) O'Sickey, M. J.; Lawrey, B. D.; Wilkes, G. L. *J. Appl. Polym. Sci.* **2002**, *84*, 229−243.
(66) Klinedinst, D. B.; Yilgör, E.; Yilgör, I.; Beyer, F. L.; Wilkes, G. L. *Polymer* **2005**, *46*, 10191−10201.
(67) O'Sickey, M. J.; Lawrey, B. D.; Wilkes, G. L. *Polymer* **2002**, *43*, 7399−7408.
(68) Gimenez, J.; Cassagnau, P.; Michel, A. *J. Rheol.* **2000**, *44* (3), 527−547.
(69) Ferry, J. D.; *Viscoelastic Properties of Polymers*; John Wiley: New York, 1980.
(70) te Nijenhuis, K. In *Springer Handbook of Experimental Fluid Mechanics*; Tropea, C., Foss, J. F., Yarin, A., Eds.; Springer-Verlag: Berlin, 2007; Chapter C1, in press.
(71) Dankers, P. Y. W.; Zhang, Z.; Wisse, E.; Grijpma, D. W.; Sijbesma, R. P.; Feijen, J.; Meijer, E. W. *Macromolecules* **2006**, *39* (25), 8763−8771.
(72) Coleman, M. M.; Skrovanek, D. J.; Hu, J.; Painter, P. C. *Macromolecules* **1988**, *21* (1), 59−65.
(73) Yamauchi, K.; Lizotte, J. R.; Hercules, D. M.; Vergne, M. J.; Long, T. E. *J. Am. Chem. Soc.* **2002**, *124* (29), 8599−8604.
(74) te Nijenhuis, K. *Macromol. Chem.* **1991**, *192*, 603−616.
(75) te Nijenhuis, K. *Macromol. Chem. Macromol. Symp.* **1991**, *45*, 117−126.
(76) te Nijenhuis, K. In *Macromolecules 1992, Invited Lectures of the 34th IUPAC International Symposium on Macromolecules, Prague, Czechoslovakia, 1992*; Kahovec, J., Ed.; VSP International Science Publishers: Utrecht, The Netherlands, 1993; pp 29−43.
(77) te Nijenhuis, K. *Polym. Gels Networks* **1993**, *1*, 185−198.
(78) te Nijenhuis, K. *Polym. Gels Networks* **1993**, *1*, 199−210.
(79) te Nijenhuis, K. *Polym. Gels Networks* **1996**, *4*, 415−433.
(80) Franse, M. W. C. P.; te Nijenhuis, K. *J. Mol. Struct.* **2000**, *554*, 1−10.
(81) Franse, M. W. C. P.; te Nijenhuis, K. *Macromol. Theory Simul.* **2002**, *11*, 342−351.
(82) te Nijenhuis, K.; *Adv. Polym. Sci.* **1997**, *130*, 1−267.
(83) Franse, M. W. C. P. Ph.D. Thesis, Technische Universiteit Delft: Delft, The Netherlands, 2002.
(84) Franse, M. W. C. P.; te Nijenhuis, K.; Groenewold, J.; Picken, S. J. *Macromolecules* **2004**, *37* (20), 7839−7845.
(85) Jonkheijm, P.; van der Schoot, P.; Schenning, A. P. H.; Meijer, E. W. *Science* **2006**, *313*, 80−83.

MA0712394